

# Synthesis and Aqueous Colloidal Solutions of $\text{RE}_2(\text{OH})_5\text{NO}_3 \cdot n\text{H}_2\text{O}$ (RE = Nd and La)

Kyung-Hee Lee<sup>[a]</sup> and Song-Ho Byeon<sup>\*[a]</sup>

**Keywords:** Layered compounds / Rare earths / Colloids / Inclusion compounds

A new, simple route leading to layered rare-earth hydroxy nitrates was developed. The pH-independent procedure uses ethanol containing alkali-metal hydroxide (KOH, RbOH, or CsOH) as a solvothermal medium. Two new, layered rare-earth hydroxy nitrates (LRHs),  $\text{Nd}_2(\text{OH})_5\text{NO}_3 \cdot n\text{H}_2\text{O}$  and  $\text{La}_2(\text{OH})_5\text{NO}_3 \cdot n\text{H}_2\text{O}$ , were prepared by this nonaqueous solvothermal reaction. Because the RE = Nd and La members have not yet been synthesized in an aqueous system, the successful synthesis of these compounds implies the completion of the  $\text{RE}_2(\text{OH})_5\text{NO}_3 \cdot n\text{H}_2\text{O}$  (RE = rare earths) series. The typical properties of a layered structure was demonstrated by ready ion-exchange reactions between  $\text{NO}_3^-$  and some or-

ganic anions such as decanoate, decanesulfonate, and decyl sulfate. In particular, the as-synthesized hydroxide from solvothermal reaction, where the alkali-metal nitrates are partially intercalated in the interlayer gallery, form an aqueous colloidal solution under ultrasonic treatment. Hydration of the LRHs intercalated with alkali-metal salts results in the formation of colloidal LRH suspensions in water. The colloidal character of the LRH solutions is supported by the Tyndall effect, TEM, and AFM images.

(© Wiley-VCH Verlag GmbH & Co. KGaA, 69451 Weinheim, Germany, 2009)

## Introduction

Recently, a series of layered compounds consisting of pure cationic rare-earth hydroxide layers was successively reported. The layered hydroxides  $[\text{RE}_4(\text{OH})_{10}(\text{H}_2\text{O})_4]\text{A}$  (RE = rare earths, A = 2,6-naphthalenedisulfonate and 2,6-anthraquinonedisulfonate), pillared by organic disulfonates, show capability as heterogeneous catalysts in “green” chemistry.<sup>[1]</sup> A family of  $\text{RE}_2(\text{OH})_5\text{NO}_3 \cdot n\text{H}_2\text{O}$  was then synthesized under hydrothermal conditions, exhibiting a large ion-exchange capacity for a wide range of organic anions.<sup>[2]</sup> The halide analogues  $\text{RE}_8(\text{OH})_{20}\text{Cl}_4 \cdot n\text{H}_2\text{O}$  and  $\text{RE}_2(\text{OH})_5\text{Br} \cdot n\text{H}_2\text{O}$  were also presented in recent papers, demonstrating a characteristic layered structure.<sup>[3–5]</sup> Practically, these compounds of the general formula  $\text{RE}_2(\text{OH})_5\text{X} \cdot n\text{H}_2\text{O}$ , called layered rare-earth hydroxides (LRHs), correspond to  $m = 0.5$  members of the rare-earth hydroxy salts  $\text{RE}(\text{OH})_{3-m}\text{X}_m \cdot n\text{H}_2\text{O}$ , where RE = rare earths and X = interlayer anions. It is accepted that the variables in the general formula could be  $0.25 \leq m \leq 1.0$  and  $0 \leq n \leq 1.0$ .<sup>[6–8]</sup>

It was suggested that the LRH structure, particularly containing nitrate as an interlayer anion ( $\text{X} = \text{NO}_3^-$ ), seems to be kinetically favored by small rare-earth ions;

gadolinium has the limiting cationic radius for these structures.<sup>[1,2]</sup> In previous work, however, it was demonstrated that a hydrothermal reaction under controlled pH conditions or by using the precipitation method can extend the  $\text{RE}_2(\text{OH})_5\text{NO}_3 \cdot n\text{H}_2\text{O}$  family to the larger rare-earth members such as Gd, Eu, and Sm.<sup>[9,10]</sup> Nevertheless RE = Nd and La members have not yet been synthesized. They were expected to form the corresponding single phases without a  $\text{RE}(\text{OH})_3$  impurity at  $\text{pH} < 6.5$ , but no precipitate was obtained after the hydrothermal reaction was performed under such low-pH conditions. This previous study proposed that a pH independent procedure is required to synthesize pure RE = Nd and La members. In the present work, we developed a nonaqueous solvothermal route to obtain a complete rare-earth  $\text{RE}_2(\text{OH})_5\text{NO}_3 \cdot n\text{H}_2\text{O}$  family. Here we report that  $\text{La}_2(\text{OH})_5\text{NO}_3 \cdot n\text{H}_2\text{O}$  and  $\text{Nd}_2(\text{OH})_5\text{NO}_3 \cdot n\text{H}_2\text{O}$  were successfully synthesized by using ethanol containing alkali-metal hydroxides as a solvothermal medium. A typical host–guest reaction of the obtained compounds was demonstrated by ion exchange of interlayer nitrate molecules with some organic anions such as decanoate, decanesulfonate, and decyl sulfate. Interestingly, the as-synthesized hydroxides from solvothermal reactions, where the alkali-metal nitrates are partially intercalated in the interlayer gallery, formed a transparent colloidal suspension in water under ultrasonication. The behavior of aqueous colloidal solutions of the obtained layered hydroxy nitrates was also investigated in this work.

[a] Department of Applied Chemistry, College of Applied Science, Kyung Hee University, Gyeonggi 446-701, South Korea  
Fax: +82-31-202-7337  
E-mail: shbyun@khu.ac.kr

Supporting information for this article is available on the WWW under <http://dx.doi.org/10.1002/ejic.200900635>.

## Results and Discussion

The nonaqueous solvothermal route is very simple and accordingly adoptable for the synthesis of a complete rare-earth series of  $\text{RE}_2(\text{OH})_5\text{NO}_3 \cdot n\text{H}_2\text{O}$ . Although the precursors of rare earths,  $\text{RE}(\text{NO}_3)_3 \cdot 6\text{H}_2\text{O}$  ( $\text{RE} = \text{Nd}$  and  $\text{La}$ ), were used without removal of hydrated water, no significant difference was observed in the yield and purity of the products. Despite extensive changes to the temperature and time of the reaction and aging, we were unable to produce single crystals of any member of the  $\text{RE}_2(\text{OH})_5\text{NO}_3 \cdot n\text{H}_2\text{O}$  family.

### Synthesis and Ion-Exchange Reaction of LNdH

$\text{Nd}_2(\text{OH})_5\text{NO}_3 \cdot n\text{H}_2\text{O}$  (LNdH) could be prepared by using KOH, RbOH, or CsOH as a hydroxide source. Before the products obtained from the solvothermal reaction for LNdH were washed with water, the corresponding nitrate form  $\text{ANO}_3$  ( $\text{A} = \text{K}, \text{Rb}, \text{or Cs}$ ) was observed as an impurity phase, and we call these compounds  $\text{Nd}_2(\text{OH})_5\text{NO}_3 \cdot \text{ANO}_3$  in this paper. Their powder X-ray diffraction (XRD) patterns are compared in Figure 1a–c. Except for the reflections related to such impurities, strong (00 $l$ ) reflections reveal the characteristics of a typical layered phase. It is of interest that the observed interlayer separation increases from 11.7 to 12.0 and 12.4 Å when the hydroxide source is changed from KOH to RbOH and CsOH, respectively. The systematic shift of the (00 $l$ ) reflections as a function of the size of the alkali-metal cations suggests that the alkali-metal salts are included in the interlayer space of the layered host compounds. Alkoxide anion co-intercalated layered double hydroxides (LDHs) have been reported in the literature.<sup>[11]</sup> In those compounds, the alkoxy groups were arranged in the interlayer space with the alkyl chains parallel to the LDH layers. Accordingly, the basal spacings showed no systematic dependence on the chain length of the alkoxide. Because the basal spacing of our products is considerably dependent on the alkali metals, it is unlikely that the ethoxide anions are intercalated. Although the inclusion of neutral alkali-metal ethoxide cannot be ruled out, the basal spacing appears too large to be attributed to the parallel orientation of the ethoxy group in the gallery. Unfortunately, attempts to isolate pure phases containing the alkali-metal salts in the interlayer space were unsuccessful. When we washed these mixed phases with water to remove the  $\text{ANO}_3$  impurity, the same compound was returned regardless of the kind of alkali-metal cation ( $\text{A}^+$ ). As shown in Figure 1d, the layered structure is retained, as evidenced by the observation of strong (00 $l$ ) reflections, but the interlayer spacing was significantly reduced to 8.4 Å after washing with water. Such an interlayer separation is comparable with those of other members of the  $\text{RE}_2(\text{OH})_5\text{NO}_3 \cdot n\text{H}_2\text{O}$  family.<sup>[2,9,10]</sup> Thus, the alkali-metal salt included in the interlayer space seems to be easily dissolved out by the water to yield a hydrated form. The composition of LNdH was determined to be  $\text{Nd}_2(\text{OH})_5\text{NO}_3 \cdot \text{H}_2\text{O}$  ( $n \approx 1.0$ ) by inductively coupled plasma (ICP) analysis and elemental analysis (EA); no alkali-metal component was detected, as summarized in Table 1.

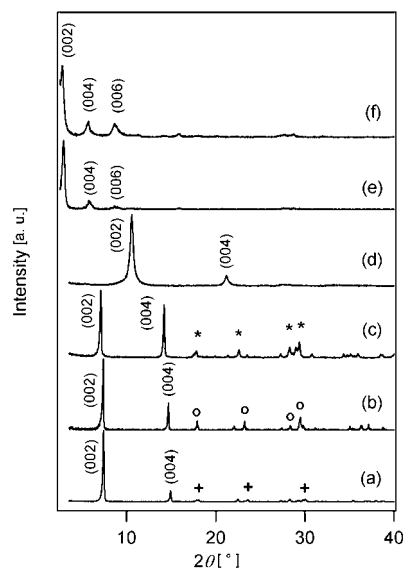


Figure 1. Powder X-ray diffraction patterns of (a)  $\text{Nd}_2(\text{OH})_5\text{NO}_3 \cdot \text{KNO}_3$  (+:  $\text{KNO}_3$  impurity), (b)  $\text{Nd}_2(\text{OH})_5\text{NO}_3 \cdot \text{RbNO}_3$  (o:  $\text{RbNO}_3$  impurity), (c)  $\text{Nd}_2(\text{OH})_5\text{NO}_3 \cdot \text{CsNO}_3$  (\*:  $\text{CsNO}_3$  impurity), (d)  $\text{Nd}_2(\text{OH})_5\text{NO}_3 \cdot n\text{H}_2\text{O}$ , (e)  $\text{Nd}_2(\text{OH})_5(\text{decanoate}) \cdot n\text{H}_2\text{O}$ , and (f)  $\text{Nd}_2(\text{OH})_5(\text{decanesulfonate}) \cdot n\text{H}_2\text{O}$ .

Table 1. Elemental analysis data for the layered rare-earth hydroxides,  $\text{RE}_2(\text{OH})_5\text{NO}_3 \cdot n\text{H}_2\text{O}$ .

Composition	Elemental analysis [%]		Basal spacing [Å]
	calcd.	found	
LNdH $\text{Nd}_2(\text{OH})_5\text{NO}_3 \cdot \text{H}_2\text{O}$	Nd 63.6 N 3.1 H 1.5	Nd 62.6 N 2.8 H 1.4	8.4
LLaH $\text{La}_2(\text{OH})_5\text{NO}_3 \cdot 1.5\text{H}_2\text{O}$	La 61.5 N 3.1 H 1.8	La 62.4 N 2.9 H 1.8	9.2

The interlayer  $\text{NO}_3^-$  ions were readily exchanged with the organic anions at room temperature. As an example, the XRD patterns of LNdHs exchanged with decanoate and decanesulfonate are compared with that of the host LNdH compound in Figure 1e,f, respectively. The replacement of  $\text{NO}_3^-$  by the organic anions could be confirmed by the disappearance of characteristic reflections attributed to the pristine host lattice (Figure 1d). All the XRD patterns show a series of intense basal (00 $l$ ) reflections after the anion exchange. As expected for a host–guest reaction, a systematic shift of these reflections towards lower diffraction angles is associated with the expansion of the interlayer separation from 8.4–30.0 Å and 30.7 Å by exchange reactions with the decanoate and decanesulfonate ions, respectively. Such a significant expansion demonstrates the incorporation of long-chain alkyl anions into the interlayer galleries of LNdH.

Figure 2 compares the thermogravimetry (TG) curve of LNdH with those of the decanoate- and decanesulfonate-exchanged derivatives. The amount of co-intercalated water

was determined from the weight loss below 150 °C. Because the ignition of prepared compounds above 700 °C yields  $\text{Nd}_2\text{O}_3$ , the observed total weight losses of 26.8, 47.2, and 48.6% are close to the losses of 25.8, 45.9, and 48.3% calculated from the chemical formula,  $\text{Nd}_2(\text{OH})_5\text{NO}_3 \cdot \text{H}_2\text{O}$ ,  $\text{Nd}_2(\text{OH})_5(\text{C}_{10}\text{H}_{21}\text{SO}_3) \cdot 1.5\text{H}_2\text{O}$ , and  $\text{Nd}_2(\text{OH})_5(\text{C}_9\text{H}_{19}\text{CO}_2)(\text{C}_9\text{H}_{19}\text{CO}_2\text{H})_{0.55} \cdot \text{H}_2\text{O}$ , respectively. An intercalation of excess carboxylic acid was also observed after an exchange reaction with other carboxylates in a previous study.<sup>[9]</sup> As a result of strong lateral dispersion interactions between long-chain alkyl ions, an inclusion exceeding the exchange capacity is often induced.<sup>[12,13]</sup>

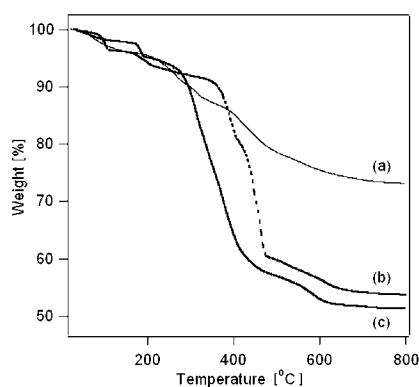


Figure 2. TG analysis curves of (a)  $\text{Nd}_2(\text{OH})_5\text{NO}_3 \cdot n\text{H}_2\text{O}$ , (b)  $\text{Nd}_2(\text{OH})_5(\text{decanesulfonate}) \cdot n\text{H}_2\text{O}$ , and (c)  $\text{Nd}_2(\text{OH})_5(\text{decanoate}) \cdot n\text{H}_2\text{O}$ .

### Synthesis and Ion-Exchange Reaction of LLaH

In contrast to LNdH that was synthesized by using any member of AOH (A = K, Rb, and Cs), the crystallinity, purity, and yield of synthesized  $\text{La}_2(\text{OH})_5\text{NO}_3 \cdot n\text{H}_2\text{O}$  (LLaH) were significantly different from one another, depending on the sort of selected alkali-metal hydroxide. The most reproducible single phase was obtained when we used the ethanol solution containing CsOH as a hydroxide source. Except for differences in synthetic conditions, other behaviors of LLaH and its derivatives were similar to those described for LNdH derivatives. As shown in the XRD pattern in Figure 3a,  $\text{CsNO}_3$  was observed as an impurity phase in the as-synthesized phase from the solvothermal reaction. The interlayer separation of 12.4 Å, calculated from the (00 $l$ ) reflections, indicates the existence of  $\text{CsNO}_3$  in the interlayer space of LLaH. Purely hydrated form of LLaH was easily obtained by washing out  $\text{CsNO}_3$  with water. As shown in Figure 3b, the layered structure is retained, as evidenced by the observation of strong (00 $l$ ) reflections, but the interlayer spacing was largely reduced to 9.2 Å after washed with water. The chemical formula of LLaH, determined by ICP and elemental analysis, was  $\text{La}_2(\text{OH})_5\text{NO}_3 \cdot 1.5\text{H}_2\text{O}$  ( $n \approx 1.5$ ) (Table 1). It was found that the interlayer spacing is significantly influenced by the amount of interlayer water.

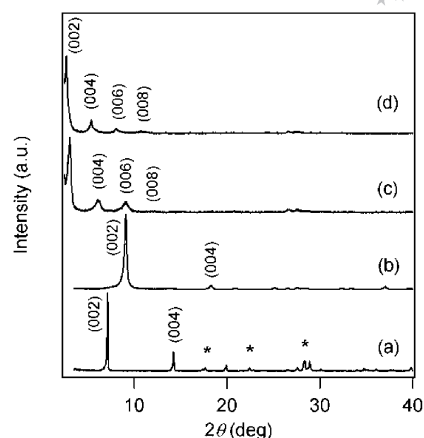


Figure 3. Powder X-ray diffraction patterns of (a)  $\text{La}_2(\text{OH})_5\text{NO}_3 \cdot \text{CsNO}_3$  (\*:  $\text{CsNO}_3$  impurity), (b)  $\text{La}_2(\text{OH})_5\text{NO}_3 \cdot n\text{H}_2\text{O}$ , (c)  $\text{La}_2(\text{OH})_5(\text{decanoate}) \cdot n\text{H}_2\text{O}$ , and (d)  $\text{La}_2(\text{OH})_5(\text{decyl sulfate}) \cdot n\text{H}_2\text{O}$ .

Figure 3c,d show the XRD patterns of decanoate and decyl sulfate exchanged LLaHs, respectively. Coupled with the absence of reflections from the pristine host lattice, well-developed (00 $l$ ) reflections demonstrate an excellent ion exchange between nitrate anion and organic carboxylate or sulfate in the galleries of LLaH. The expansion of the interlayer space from 9.2 to 29.0 and 32.7 Å also supports the intercalation of decanoate and decyl sulfate ions into the interlayer space. As in the case of LNdH-related compounds, the amount of interlayer water was determined from the weight loss below 150 °C (see the Supporting Information, Figure S1, for TG curves of LLaH and its derivatives). Considering that  $\text{La}_2\text{O}_3$  is finally obtained after heating the prepared compounds above 700 °C, the expected losses of 27.9, 48.1, and 49.8% for the chemical formula  $\text{La}_2(\text{OH})_5\text{NO}_3 \cdot 1.5\text{H}_2\text{O}$ ,  $\text{La}_2(\text{OH})_5(\text{C}_{10}\text{H}_{21}\text{OSO}_3) \cdot 1.5\text{H}_2\text{O}$ , and  $\text{La}_2(\text{OH})_5(\text{C}_9\text{H}_{19}\text{CO}_2)(\text{C}_9\text{H}_{19}\text{CO}_2\text{H})_{0.60} \cdot \text{H}_2\text{O}$  were in agreement with the observed total weight loss of 29.0, 48.6, and 48.8%, respectively.

### SEM Images and SAED Patterns of LNdH and LLaH

The morphologies of LNdH and LLaH were examined. As can be seen from the SEM images in Figure 4a,b, they comprise plate-like microcrystalline powders (see the Supporting Information, Figure S2, for SEM images of the organic anion-exchanged derivatives). Because of the very weak intensity and insufficient number of non-(00 $l$ ) reflections observed in the XRD patterns of LNdH and LLaH, the arrangement mode within the  $ab$  plane was measured by the selected area electron diffraction (SAED). As shown in Figure 4c,d, the clear spots, which are rectangularly arranged, indicate an order within the  $ab$  plane of the LRHs. The spots assigned to (040), (220), and (400) reflections are consistent in the reciprocal lattices of the  $\text{RE}_2(\text{OH})_5\text{-X} \cdot n\text{H}_2\text{O}$  family.<sup>[2,3-5,9,10]</sup> The determined lattice parameters are  $a = 0.75, 0.76$  nm and  $b = 1.34, 1.36$  nm for LNdH and LLaH, respectively.

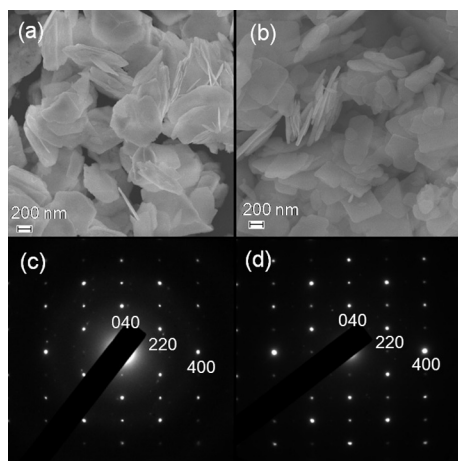


Figure 4. FE-SEM images and selected-area electron diffraction patterns of (a and c)  $\text{Nd}_2(\text{OH})_5\text{NO}_3 \cdot n\text{H}_2\text{O}$  and (b and d)  $\text{La}_2(\text{OH})_5\text{NO}_3 \cdot n\text{H}_2\text{O}$ .

### IR Spectra of LNdh and LLaH and Their Organic Anion-Exchanged Derivatives

The complete exchange reaction between nitrate ion and organic anion was monitored with IR spectroscopy. The FTIR spectra of LNdh and LLaH host materials are compared with those of the organic anion-exchanged derivatives in Figure 5. The characteristic O–H stretching vibrations expected for the hydroxide layer and the interlayer water are observed at  $3400\text{--}3600\text{ cm}^{-1}$  for all the measured compounds.<sup>[14]</sup> The medium intensity band close to  $1635\text{ cm}^{-1}$  is due to the well-known bending mode of interlayer water molecules. The strong band at  $1380\text{ cm}^{-1}$  in the spectra of LNdh (Figure 5a) and LLaH (Figure 5b) is assigned to the  $\nu_3$  vibration mode of the  $\text{NO}_3^-$  ions.<sup>[15,16]</sup> After anion-exchange reactions, several absorption bands attributed to the interlayer organic anions are observed. Absorptions at around  $1534$  and  $1442\text{ cm}^{-1}$  in the IR spectra of  $\text{La}_2(\text{OH})_5(\text{decanoate}) \cdot \text{H}_2\text{O}$  (Figure 5c) are due to the asymmetric and

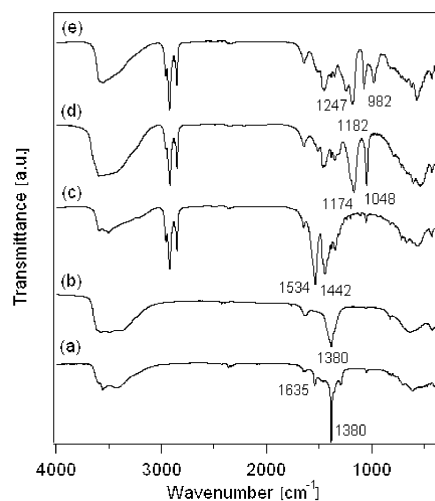


Figure 5. FTIR spectra of (a)  $\text{Nd}_2(\text{OH})_5\text{NO}_3 \cdot n\text{H}_2\text{O}$ , (b)  $\text{La}_2(\text{OH})_5\text{NO}_3 \cdot n\text{H}_2\text{O}$ , (c)  $\text{La}_2(\text{OH})_5(\text{decanoate}) \cdot n\text{H}_2\text{O}$ , (d)  $\text{Nd}_2(\text{OH})_5(\text{decanesulfonate}) \cdot n\text{H}_2\text{O}$ , and (e)  $\text{La}_2(\text{OH})_5(\text{decyl sulfate}) \cdot n\text{H}_2\text{O}$ .

symmetric stretching modes of the  $\text{COO}^-$  group, respectively.<sup>[15]</sup> The  $\text{SO}_3^-$  group shows also two typical bands, an asymmetric stretch at  $1174\text{ cm}^{-1}$  and a symmetric stretching mode at  $1048\text{ cm}^{-1}$  in the spectrum of  $\text{Nd}_2(\text{OH})_5(\text{decanesulfonate}) \cdot \text{H}_2\text{O}$  (Figure 5d).<sup>[12,17]</sup> The broad and sharp absorptions at  $1182\text{--}982$  and  $1247\text{ cm}^{-1}$  in Figure 5e correspond to the S–O symmetric and asymmetric stretching vibrations of the sulfate group in  $\text{La}_2(\text{OH})_5(\text{decyl sulfate}) \cdot \text{H}_2\text{O}$ , respectively.<sup>[5,18–20]</sup> Such observations of characteristic bands for carboxylate, sulfonate, and sulfate groups confirm the intercalation of the corresponding organic anions into the interlayer space of LNdh and LLaH.

### Aqueous Colloidal Suspensions of LNdh and LLaH

One of the interesting features of LNdh and LLaH containing  $\text{ANO}_3$  ( $A = \text{K}, \text{Rb}, \text{or Cs}$ ) in the interlayer space is the fact that the supernatant solution formed a transparent colloidal suspension when they were dispersed in water by ultrasonication. In contrast, the hydrated forms of LNdh and LLaH did not produce a colloidal solution even after severe ultrasonication. Such a difference indicates that the interlayer alkali-metal salt plays an important role in the formation of an aqueous colloidal solution. It could be accordingly proposed that an inclusion of excess water to hydrate the alkali-metal salt in the interlayer space would partially delaminate the LRHs to yield a colloidal suspension. A complete delamination should be further investigated. As can be seen from Figure 6a,b, laser illumination of the suspensions obtained after removing the particles precipitated by centrifugation shows the Tyndall effect, thus suggesting the presence of abundant particles dispersed in water. Typi-

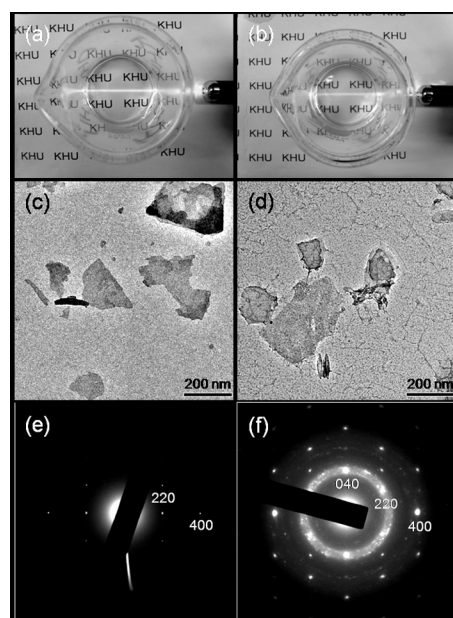


Figure 6. Photographs of the aqueous colloidal suspensions of (a) LNdh and (b) LLaH; a light beam was irradiated from the side to demonstrate the Tyndall effect (c and d); TEM images and (e and f) SAED patterns of LNdh and LLaH sheets in aqueous colloidal solutions, respectively.



cal transmission electron microscopy (TEM) images taken from randomly chosen particles in aqueous colloidal solutions of LNdH and LLaH show ultrathin sheets (Figure 6c,d). The SAED patterns measured during the TEM study displayed ( $hk0$ ) spots, depicting the crystalline nature of the nanosheets (Figure 6e,f). Their rectangular arrangement is consistent with those of pristine LNdH and LLaH (Figure 4). In particular, the spots assigned to the (040), (220), and (400) reflections are accounted for by essentially the same reciprocal lattice ( $a \approx 0.75$  nm,  $b \approx 1.35$  nm). Thus, it can be proposed that the intralayer structure of LNdH and LLaH remains unchanged in aqueous colloidal suspension.

The size and thickness of the nanosheets in colloidal solutions were further examined by atomic force microscopy (AFM). The clear dispersion in water was deposited on a freshly cleaved mica substrate. The AFM image over a large scanning area (Figure 7a,b) displays well-dispersed nanoparticles on the substrate surface. The particles are sheet-like with a lateral dimension of typically 50–300 nm, which is close to that observed in the TEM image. The height profiles along the white lines marked in Figure 7c,d show a thicknesses of about 2 and 4–8 nm for the nanosheets of LNdH and LLaH, respectively. Considering the

basal spacings of 0.84–0.92 nm, it can be proposed that the nanosheets in the suspension consist of mainly three to eight monolayers.

## Conclusions

A new, simple method was developed to synthesize layered rare-earth hydroxy nitrates, where ethanol containing alkali-metal hydroxides was used as a solvothermal medium. We could complete the  $\text{RE}_2(\text{OH})_5\text{NO}_3 \cdot n\text{H}_2\text{O}$  family for the rare-earth series by synthesizing  $\text{La}_2(\text{OH})_5\text{NO}_3 \cdot n\text{H}_2\text{O}$  and  $\text{Nd}_2(\text{OH})_5\text{NO}_3 \cdot n\text{H}_2\text{O}$  under these nonaqueous solvothermal conditions. High yield and reproducibility of the pH-independent procedure can be extended to other rare-earth members. In particular, the as-synthesized phases including alkali-metal nitrates in their interlayer space can form a transparent aqueous colloidal suspension. Nanosheets in the colloidal solution of the layered rare-earth hydroxy nitrates will be of interest for the fabrication of rare-earth films and reconstruction of nanostructured or nanohybrid rare-earth materials.

## Experimental Section

**Synthesis of LNdH and LLaH:** For the syntheses of layered neodymium hydroxy nitrate (LNdH) and layered lanthanum hydroxy nitrate (LLaH),  $\text{RE}(\text{NO}_3)_3 \cdot 6\text{H}_2\text{O}$  (RE = Nd and La) (ca. 1.5 mmol) was dissolved in ethanol (35 mL). The obtained solution was then added to ethanol (35 mL) containing AOH [A = K, Rb, and Cs; molar ratio  $\text{AOH}/\text{RE}(\text{NO}_3)_3 \cdot 6\text{H}_2\text{O}$ , 2:1] under vigorous stirring at room temperature. Although AOH was not completely dissolved in this ethanol solution at room temperature, AOH was dissolved during the successive solvothermal reaction. The resulting mixture was put into a Teflon-lined stainless steel autoclave with a capacity of 100 mL. The sealed autoclave was maintained at 150–160 °C for 16 h. The solution was continuously stirred during the solvothermal treatment. After completion of the reaction, the solid product was collected by filtration, washed with ethanol several times, and dried at room temperature. At this stage,  $\text{ANO}_3$  was formed as an impurity phase, and the interlayer separations of the products were different depending on the size of the alkali-metal cations (see Results and Discussion). To obtain pure layered hydroxides, these mixtures were washed with deionized water and dried at 40 °C for a day.

**Ion-Exchange Reactions:** In a typical ion-exchange reaction, LNdH or LLaH powder (0.25 g) was dispersed into an aqueous anionic solution containing a threefold molar excess of decyl sulfonate ( $\text{C}_{10}\text{H}_{21}\text{SO}_3^-$ ), decyl sulfate ( $\text{C}_{10}\text{H}_{21}\text{OSO}_3^-$ ), or decanoate ( $\text{C}_9\text{H}_{19}\text{CO}_2^-$ ) sodium salts. The exchange between  $\text{NO}_3^-$  and organic anions was carried out at room temperature for 10 h in air while stirring. The resulting precipitate was recovered by filtration, washed with water, and dried at 40 °C.

**Aqueous Colloidal Solutions:** To prepare an aqueous colloidal suspension, a portion of the  $\text{ANO}_3$  intercalated LNdH or LLaH slurry was dispersed in deionized water and ultrasonicated in successive intervals of 10 min. A colloidal solution with relatively high turbidity was yielded after 1 h at room temperature. The supernatant transparent colloidal suspension was obtained after removing the precipitated particles by centrifugation. No sedimentation was de-

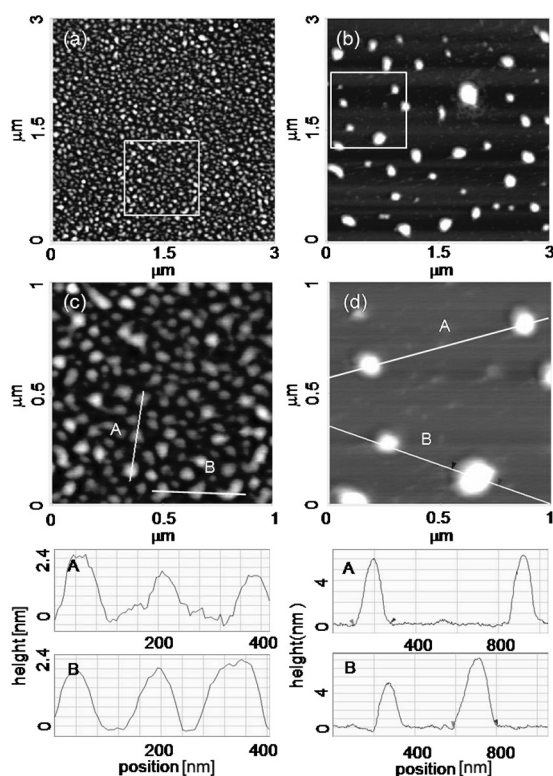


Figure 7. AFM images of (a)  $\text{Nd}_2(\text{OH})_5\text{NO}_3 \cdot n\text{H}_2\text{O}$  and (b)  $\text{La}_2(\text{OH})_5\text{NO}_3 \cdot n\text{H}_2\text{O}$  nanosheets deposited on mica. Nanosheets were randomly selected from the corresponding aqueous colloidal suspensions. The images in the white squares are enlarged in (c) and (d), respectively. The height profiles were measured along the white lines A and B in (c) and (d).

tected when the aqueous colloidal suspensions of LNdH and LLaH were left to stand for several days at room temperature.

**Characterization:** The powder X-ray diffraction pattern was recorded with a rotating anode installed diffractometer (MacScience Model M18XHF). The Cu- $K_{\alpha}$  radiation used was monochromated by a curved-crystal graphite. Field emission scanning electron microscopy (FE-SEM) was carried out with a Carl Zeiss LEO SUPRA electron microscope operating at 30 kV. Transmission electron microscopy (TEM) and selected area electron diffraction (SAED) observations were made with a JEOL JEM-2100F electron microscope operating at 300 kV. The composition of the prepared compounds was determined by elemental analysis (CE Instruments Flash EA1112), thermogravimetry (Seiko Instruments TG/DTA320), and inductively coupled plasma (Thermo Elemental Thermo ICAP 6000) analysis. Fourier transform infrared (FTIR) spectra in the range 400–4000  $\text{cm}^{-1}$  were measured with a JASCO FT/IR-4200 infrared spectrophotometer using the KBr pellet technique. A nominal resolution was 4  $\text{cm}^{-1}$ . Atomic force microscopy (AFM) was carried out by using Pucostation STD. A clear dispersion in water and formamide was deposited on a freshly cleaved mica substrate.

**Supporting Information** (see also the footnote on the first page of this article): TG curves of LLaH and its derivatives; SEM images of the organic anion-exchanged derivatives.

## Acknowledgments

This research was supported by the Korea Science and Engineering Foundation (KOSEF) through grant R01-2008-000-10442-0.

- [1] F. Gandara, J. Perles, N. Snejko, M. Iglesias, B. Gomez-Lor, E. Gutierrez-Puebla, M. Angeles Monge, *Angew. Chem. Int. Ed.* **2006**, *45*, 7998–8001.
- [2] L. J. McIntyre, L. K. Jackson, A. M. Fogg, *Chem. Mater.* **2008**, *20*, 335–340.
- [3] F. Geng, Y. Matsushita, R. Ma, H. Xin, M. Tanaka, F. Izumi, N. Iyi, T. Sasaki, *J. Am. Chem. Soc.* **2008**, *130*, 16344–16350.
- [4] L. Poudret, T. J. Prior, L. J. McIntyre, A. M. Fogg, *Chem. Mater.* **2008**, *20*, 7447–7453.
- [5] F. Geng, H. Xin, Y. Matsushita, R. Ma, M. Tanaka, F. Izumi, N. Iyi, T. Sasaki, *Chem. Eur. J.* **2008**, *14*, 9255–9260.
- [6] J. M. Haschke, *J. Solid State Chem.* **1975**, *12*, 115–121.
- [7] J. M. Haschke, L. Eyring, *Inorg. Chem.* **1971**, *10*, 2267–2274.
- [8] F. L. Carter, S. Levinson, *Inorg. Chem.* **1969**, *8*, 2788–2791.
- [9] K.-H. Lee, S.-H. Byeon, *Eur. J. Inorg. Chem.* **2009**, 929–936.
- [10] S. A. Hindocha, L. J. McIntyre, A. M. Fogg, *J. Solid State Chem.* **2009**, *182*, 1070–1074.
- [11] E. Gardner, K. M. Huntoon, T. J. Pinnavaia, *Adv. Mater.* **2001**, *13*, 1263–1266.
- [12] R. Trujillano, M. J. Holgado, F. Pigazo, V. Rives, *Phys. B* **2006**, *373*, 267–273.
- [13] G. R. Williams, D. O'Hare, *Solid State Sci.* **2006**, *8*, 971–980.
- [14] F. M. Labajos, V. Rives, M. A. Ulibarri, *J. Mater. Sci.* **1992**, *27*, 1546–1552.
- [15] K. Nakamoto, *Infrared and Raman Spectra of Inorganic and Coordination Compounds*, 4th ed., Wiley, New York, **1986**.
- [16] H. C. Zeng, Z. P. Xu, M. Qian, *Chem. Mater.* **1998**, *10*, 2277–2283.
- [17] R. Trujillano, M. J. Holgado, J. L. González, V. Rives, *Solid State Sci.* **2005**, *7*, 931–935.
- [18] L. Mohanambe, S. Vasudevan, *J. Phys. Chem. B* **2006**, *110*, 14345–14354.
- [19] Q. Z. Yang, D. J. Sun, C. Z. Zhang, X. J. Wang, W. A. Zhao, *Langmuir* **2003**, *19*, 5570–5574.
- [20] R. A. MacPhail, H. L. Strauss, R. G. Snyder, C. A. Elliger, *J. Phys. Chem.* **1984**, *88*, 334–341.

Received: July 6, 2009

Published Online: September 21, 2009